

# TENSILE STRENGTH OF C/C COMPOSITES

Jun Koyanagi\*, Hiroshi Hatta\*, Yasuo Kogo\*\*, Ichiro Shiota\*\*\*

\*Institute of Space and Astronautical Science, Japan Aerospace Exploration Agency,

\*\*Department of Materials Science and Technology, Tokyo University of Science

\*\*\* Department of Materials Science and Technology, Kogakuin University

**Keywords:** *C/C composites, tensile strength, fracture mechanism*

## ABSTRACT

*Fracture mechanism and model based on it in Carbon-carbon composites are studied. Interfacial strength between reinforcing fiber and matrix is a potential candidate governing the tensile fracture of C/Cs. However, The mechanisms connecting the tensile strength and the factor have not yet been clarified. In the present study, tensile fracture patterns of various C/C composites with changing the interfacial strength were observed in detail, and a fundamental tensile fracture model of C/C composites in accordance with the experimental observations were proposed. The analytical result shows reasonable agreement with the experimental results, and verifies that the fracture mechanism is consistent.*

## 1. INTRODUCTION

Because of unique high specific strength and stiffness in high temperature environments above 2000 °C, carbon fiber reinforced carbon matrix composites (C/Cs) are expected to expand the application to high temperature structures especially expected in the aerospace fields. In such applications, it is an import premise for reliable material and structural designs that fracture mechanisms are clearly understood, and strengths are designable. Fracture mechanisms and quantitative model of C/Cs, however, remain not clarified, even though most fundamental behavior of tensile fracture under a load in a fiber direction.

Recently, present authors reported that tensile strengths of various C/Cs are clearly understood by the effects of the fiber/matrix interfacial strength and strength distribution of reinforcing carbon fiber [1-3]. However, we could not specify the mechanisms affecting the interfacial strength on tensile strength of C/Cs, of course neither did quantitative model. In the present study, C/Cs possessing systematically varying interfacial strength were prepared by

changing heat treatment temperature, and the tensile strength and interfacial strength were measured. In addition, comparing these results with their fracture patterns, a tensile fracture model of C/Cs was proposed.

## 2. EXPERIMENTAL PROCEDURE

### 2.1 Materials

Two types of C/Cs were examined. These C/Cs were different only in their reinforcing fibers, K321 and K633 by Mitsubishi Sanshi Co. Japan. These fibers were fabricated from the same precursor but differed only in HTT. Hereafter, the C/Cs reinforced with K321 and K633 will be referred to as K321-C/C and K633-C/C, respectively. Both C/Cs were of a symmetric 0°/90° cross-ply lamination, fabricated from carbon fiber reinforced phenolic resin matrix composites, CFRPs, with a fiber volume fraction,  $V_f$ , of 60 %, and produced by the following steps. After the carbonization of the CFRPs at 1273 K, the resulting porous C/Cs were densified by five cycles of a hot isostatic pressuring process (HIP). The C/Cs thus obtained were finally heat-treated at various temperatures between 1273 K and 3173K. In order to discuss the tensile fracture mechanisms of the C/Cs, the mechanical properties of the constituent materials are often required as functions of HTT. For this purpose, the K321 and K633 fibers and matrix materials were also heat-treated under the same conditions as the C/Cs.

### 2.2 Tensile Tests of C/Cs

The tensile strengths and stress-strain relations of the C/Cs heat-treated at various temperatures were obtained at room temperature using strip specimens, which were of length 200 mm x width 10 mm x thickness 1.5 mm. The tensile load was applied using a screw-driven mechanical testing machine, an Autograph AG-5000A (Shimadzu Co. Japan), under a crosshead speed of 0.1 mm/min.

### 2.3 Bundle Push-out Tests

The interfacial strengths of the C/Cs were evaluated using the fiber-bundle push-out (FBP) method [2]. In this method, the periphery of a fiber bundle including about 30 fibers in a C/C was fractured by a load applied using a needle of 50  $\mu\text{m}$  in diameter, and the specimen thickness was set to approximately 100  $\mu\text{m}$ . The load was applied using a screw-driven mechanical testing machine (Orientech RTM-25, maximum load: 25kgf) under a crosshead speed of 0.1 mm/min. The interfacial debonding and sliding stresses could be determined by the FBP test. The interfacial (debonding) strength  $\tau_i$  was evaluated using the following equations:

$$\tau_i = F_{\max}/(Lt), \quad (1)$$

where the maximum load during a FBP test was denoted by  $F_{\max}$ , the debonded peripheral length of the bundle by  $L$ , and the length of the bundle (= specimen thickness) by  $t$ .

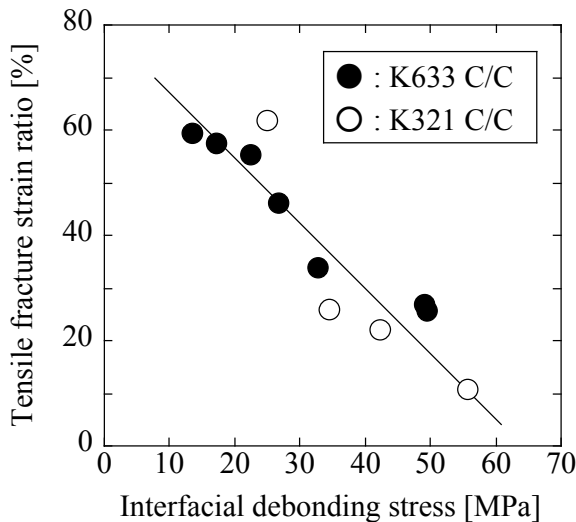


Figure 1. Tensile fracture strain ratio  $r_\epsilon$ 's ( $= \epsilon_u/\epsilon_{uf}$ 's) of K321- and K633-C/Cs as functions of interfacial debonding stress  $\tau_i$ .

## 3. RESULTS

### 3.1 Tensile strength of C/C composites

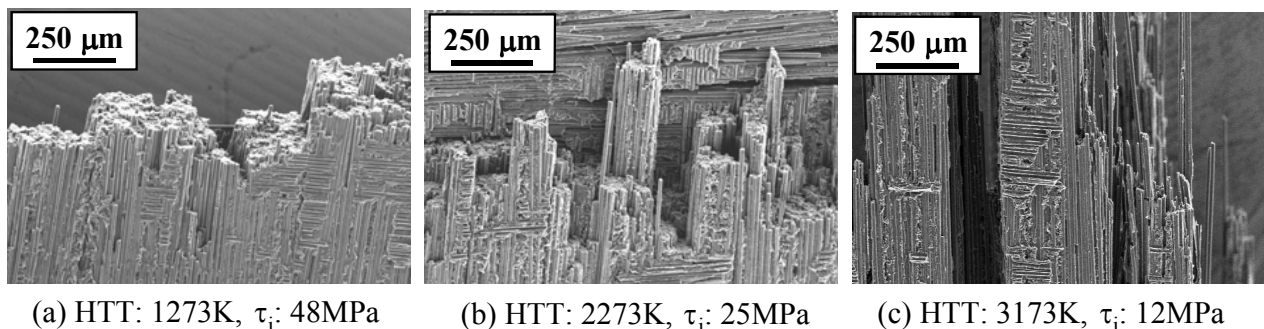
Figure 1 shows relation between  $\tau_i$  and fracture strain ratios ( $r_\epsilon$ ) of the K633- and K321-C/Cs, where  $r_\epsilon$  is defined by the ratio of experimentally determined  $\epsilon_u$  of C/C divided by experimental average value of rupture strain of the fiber  $\epsilon_{uf}$ . Thus, high  $r_\epsilon$  values imply that the potential high strength of the fiber is reflected in the composite strength. As shown in Fig. 1, when the  $\tau_i$  is high, only 10-30 % of fiber potential was exerted in tensile strength of C/Cs. To identify the mechanisms leading to such a low strength is one of objectives of the present study. Figure 1 shows that  $r_\epsilon$  improves and  $\tau_i$  decreases with increasing HTT, and nearly one curve can be drawn for different types of C/Cs. This result demonstrates that low  $\tau_i$  leads to high strength. This tendency was also obtained for resin charred and HIPed C/Cs [1].

### 3.2 Observations of fracture surfaces

Figure 2 shows SEM photographs of the fracture surfaces of the K633-C/Cs after tensile tests. These fracture surfaces are composed of brittle fractures in bundle units, and the thickness of the fracture bundles (FB) decreases with decreases in the  $\tau_i$ . This result implies that tensile fractures of the C/Cs proceeded with intermittent brittle fractures in bundle units, and the ultimate fracture occurs after an accumulation of bundle fractures.

### 3.3 Tensile fracture mechanism of C/Cs

Above data imply that the strength of a fiber-bundle-C/C should be determined by the fiber in the bundle with lowest strength. When a fiber-bundle-C/C becomes thicker, the probability of including a lower-strength fiber increases. Therefore, the strength of a fiber-bundle-C/C decreases with increased bundle thickness. Moreover, when several bundles in a C/C fracture, the surviving part of the



(a) HTT: 1273K,  $\tau_i$ : 48MPa

(b) HTT: 2273K,  $\tau_i$ : 25MPa

(c) HTT: 3173K,  $\tau_i$ : 12MPa

Figure 2. Tensile fracture surfaces of K633 heat-treated at various temperatures.

C/C supports the load that the fractured bundle previously supported. These transferred loads become larger when the thicker the fracture bundles become. These two mechanisms summarized in Figure 3 explain the tendency obtained on the tensile strength of C/Cs [1,2]: i.e., that the tensile strength of C/C decreases with increased thickness of fracture bundles, in other words, with increasing interfacial strength.

In the fracture pattern in Fig. 3, the interfaces between fracture bundles and surviving C/C is assumed to be debonded. Thus, the stress concentrations induced in surviving C/C caused by fracture bundles can be neglected. This implies that bundle fractures in a C/C occur independently without interaction between fracture bundles. Accordingly, it can be concluded that the tensile strength of C/Cs can be predicted by a model sheaving fiber-bundles in C/Cs with the same thickness distribution as a fractured C/C (e.g., Fig. 2) without mechanical interaction between the bundles. Based on this fracture mechanism, we predict the ultimate tensile strength of C/Cs in the following section.

#### 4. Theoretical model

##### 4.1 Formulation of tensile strength

A fiber failure probability at stress  $\sigma$  can be generally written by the following equation based on Weibull statistics,

$$p = 1 - \exp\left(-\frac{L}{L_0}\left(\frac{\sigma}{\sigma_0}\right)^m\right), \quad (2)$$

where  $L_0$ ,  $\sigma_0$  and  $m$  represent Weibull parameters. In this study, it is assumed that when the weakest fiber in fracture bundle consisting of  $n$  number of fibers fails, the bundle fails in time. Therefore, the failure probability of the fiber that is constitutive part of the fiber bundle consisting of  $n$  number of fibers can be written as in

$$p(n) = 1 - \exp\left(-\frac{L \cdot n}{L_0}\left(\frac{E_f \varepsilon}{\sigma_0}\right)^m\right), \quad (3)$$

where applied stress is substituted by Young's modulus of fiber  $E_f$  x applied  $\tilde{\varepsilon}$ . In fact, various

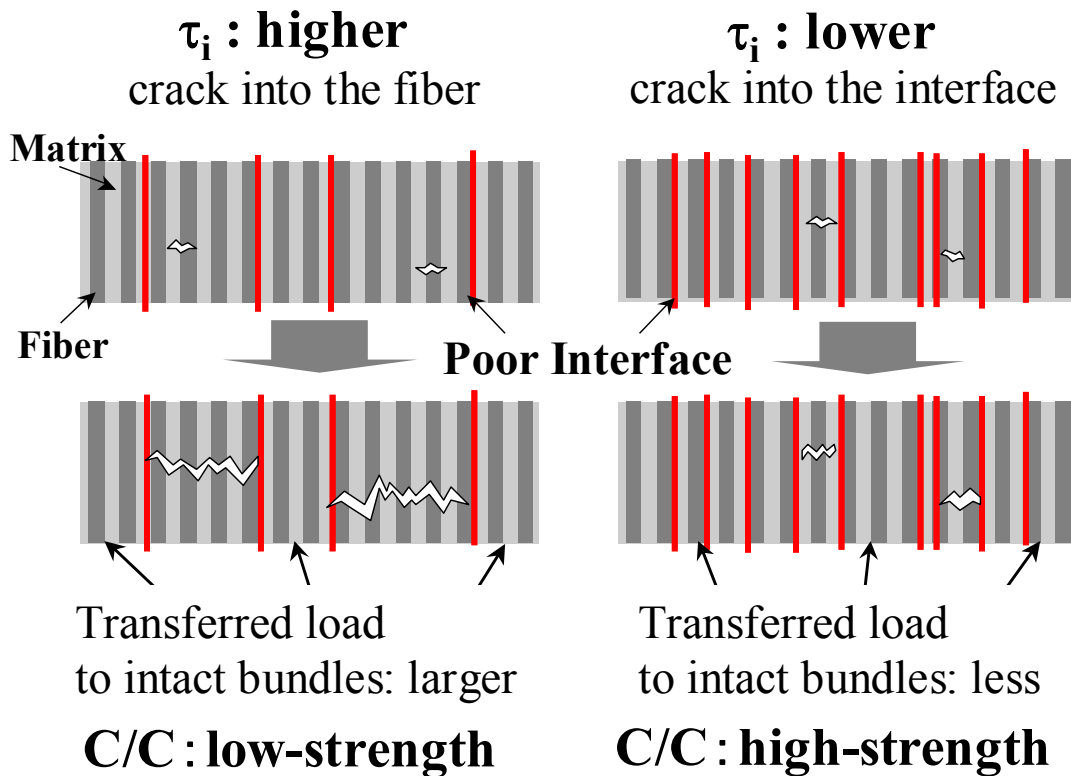


Figure 3. Fracture pattern of C/C composites

numbers of fibers compose a fiber bundle. The failure probability of all fibers can be obtained by amount of product of equation (3) and a probability  $q(n)$  that arbitrary fiber is a constitutive part of the fiber bundle consisting of  $n$  number of fibers,

$$P = \left\{ 1 - \exp\left(-\frac{L \cdot 1}{L_0} \left(\frac{E_f \varepsilon}{\sigma_0}\right)^m\right) \right\} \cdot q(1) + \left\{ 1 - \exp\left(-\frac{L \cdot 2}{L_0} \left(\frac{E_f \varepsilon}{\sigma_0}\right)^m\right) \right\} \cdot q(2) + \dots + \left\{ 1 - \exp\left(-\frac{L \cdot n}{L_0} \left(\frac{E_f \varepsilon}{\sigma_0}\right)^m\right) \right\} \cdot q(n) + \dots \quad (4)$$

Equation (4) is rewritten in

$$P = \sum_{n=1}^{\infty} \left\{ 1 - \exp\left(-\frac{n \cdot L}{L_0} \left(\frac{E_f \varepsilon}{\sigma_0}\right)^m\right) \right\} q(n) \quad (5)$$

When  $P$  is small,  $P$  can be approximated by

$$P \approx \frac{L}{L_0} \left(\frac{E_f \varepsilon}{\sigma_0}\right)^m F(n), \quad (6)$$

where

$$F(n) = \sum_{n=1}^{\infty} n \cdot q(n). \quad (7)$$

Tensile load of C/Cs is assumed to be distributed only into longitudinal fibers. The specimen stress  $\sigma_{\text{spe}}$  is described by the following equation using volume fraction of the longitudinal fiber  $V_{f,0}$  and the fiber-failure probability  $P$ .

$$\sigma_{\text{spe}} = V_{f,0} E_f \varepsilon (1 - P) \quad (8)$$

Equation (6) and (8) derive the next relationship between the specimen stress and the applied strain.

$$\sigma_{\text{spe}} = \left\{ 1 - \frac{L}{L_0} \left(\frac{E_f \varepsilon}{\sigma_0}\right)^m F(n) \right\} V_{f,0} E_f \varepsilon \quad (9)$$

Here,  $\frac{\partial \sigma_{\text{spe}}}{\partial \varepsilon} = 0$  leads a critical value of the applied strain and a maximum value of the specimen stress. These values can be identified as a rupture strain and a rupture stress, respectively. Eventually, the rupture strain and the rupture stress can be calculated as

$$\varepsilon_{\text{rup}} = \frac{\sigma_0}{E_f} \left( \frac{L(m+1)F(n)}{L_0} \right)^{-1/m} \quad \text{and} \quad (10)$$

$$\sigma_{\text{rup}} = V_{f,0} \sigma_0 \left( \frac{m}{m+1} \right) \left( \frac{L(m+1)F(n)}{L_0} \right)^{-1/m}. \quad (11)$$

As shown in equation (11), we can obtain the tensile strength of C/Cs using the Weibull parameters demonstrating the single fiber strength distribution and  $F(n)$  that implies a kind of expected number of the fracture-bundle.

## 4.2 Experimental verification

Experimentally obtained strength of K633 C/C is compared with the predicted strength using eq. (11) in Figure 4 as a function of the specific value of  $F(n)$  regarding as the thickness of fracture-bundle determined by counting whole fracture-bundle in several photos of the fracture surfaces. We use these parameters' values:  $L_0=25\text{mm}$ ,  $\sigma_0=3000\text{MPa}$ ,  $m=5.8$ ,  $V_{f,0}=0.3$ ,  $L=100\text{mm}$ . These Weibull parameters are determined by to refer the experimental data of single fiber tensile test for carbon fiber annealed at 2300K. As Fig. 4 shows, the present prediction reasonably agreed with experimental values. This result indicates that the fracture model shown in Fig.2 is consistent.

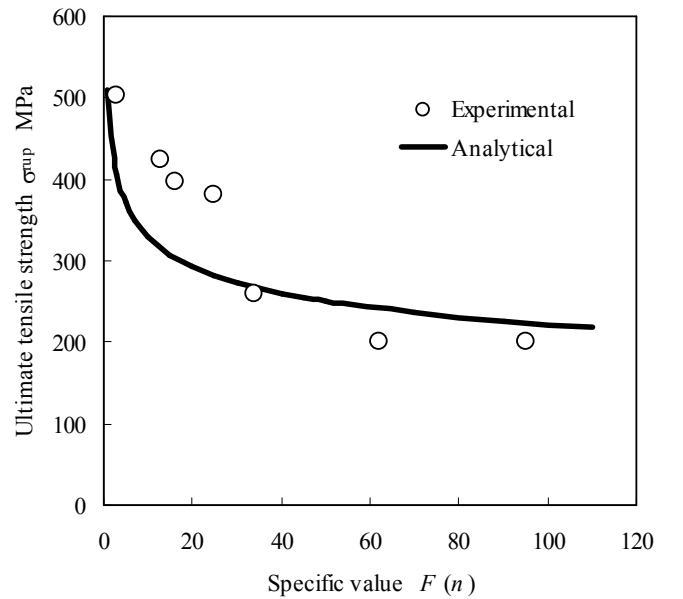


Fig. 4 Comparison analytical results and experimental results of tensile tests in C/Cs

## 5. CONCLUSION

- 1) The tensile fracture of C/Cs occurred with intermitted increase in bundle fracture.
- 2) The fracture bundle became thinner with decrease in interfacial strength between the fiber and matrix, and thinner bundle lead to higher tensile strength.
- 3) A tensile fracture model of unidirectionally reinforced C/C was proposed on the basis of experimental observations, and the predicted strengths using this model reasonably agreed with experimentally observed strengths.

## REFERENCES

- [1] Hiroshi Hatta, Keiji Suzuki, Tetsuro Shigei, Satoshi Somiya, and Yoshihiro Sawada. 2001. "Strength improvement by densification of C/C composites," Carbon, 39: 83-90.
- [2] Hiroshi Hatta, Tatsuji Aoi, Itaru Kawahara, Yasuo Kogo, and Ichiro Shiota. 2004. "Tensile strength of Carbon/Carbon composites: I - Effect of C-C Density," J. Compos. Mater. 38(19): 1667-1684.
- [3] Hiroshi Hatta, Tatsuji Aoi, Itaru Kawahara, and Yasuo Kogo. 2004. "Tensile strength of Carbon/Carbon composites: II - Effect of Heat Treatment Temperature," J. Compos. Mater. 38(19): 1685-1699.
- [4] Hiroshi Hatta, Itaru Kawahara, Yurika Goto, Jun Koyanagi and Ichiro Shiota, "Tensile Strength of Carbon/Carbon Composites, III: Effect of Heat Treatment Temperature (Pitch-Based Carbon Fiber Reinforced C/Cs), " to be submitted in Carbon.